TITLE:

Algorithm Document

Tropospheric NO_2

Authors :

R.J. van der A (KNMI)
H.J. Eskes (KNMI)
M. Van Roozendael (BIRA-IASB)
I. De Smedt (BIRA-IASB)
N. Blond (LISA)
F. Boersma (KNMI)
A. Weiss(EMPA)
J.C.A. van Peet (KNMI)

DOCUMENT STATUS SHEET

Issue	Date	Modified Items / Reason for Change
0.9	18.01.06	First Version
1.0	29.04.10	Updated version after review by J.C. Lambert

TABLE OF CONTENTS

1. INTRODUCTION

Nitrogen oxides play a central role in tropospheric chemistry, and there are several reasons why an improved knowledge of the global tropospheric distribution of NOx (NO+NO2) is important:

- NOx and volatile organic compounds are emitted in large quantities due to human activities such as traffic and industry. In the summer months this mixture produces photochemical smog.

- The chemical budget of ozone in the troposphere is largely determined by the concentration of NOx. The knowledge of the ozone distribution and its budgets is strongly limited by a severe lack of observations of NO and NO2 in the troposphere.

- The variability of NOx concentrations in the lower troposphere in industrialised areas and near biomass burning sites is very large. The few available point observations of NOx, on the ground or from aircraft measurements, are therefore difficult to translate to regional scale concentrations. The residence time of NOx in the lower troposphere is short. Therefore observations of boundary layer NOx contain important information on the emissions of nitric oxide, and the trends in these emissions.

- The free troposphere is also of great importance for the ozone budget, and for CH4 and CO oxidation processes. Again these budgets are uncertain due to a limited knowledge of NOx. The degree of NOx transfer from the boundary layer is difficult to model, and NOx emissions from lightning are very uncertain.

Formaldehyde (CH2O) is a major intermediate gas in the oxidation of methane and many other hydrocarbons. The lifetime of formaldehyde is short, and the photolysis reactions and reaction with OH form a major source of CO. Because of the short lifetime of several hours, the presence of formaldehyde signals hydrocarbon emission areas. Formaldehyde is important, since it is a measure of the total amount of oxidised hydrocarbons, and together with NOx quantifies the chemical ozone production. The presence of elevated levels of CH2O is related to the release of hydrocarbons (ethene, isoprene, and methane) by forests, biomass burning, traffic and industrial emissions.

An important step in filling the gap in our knowledge of tropospheric NOx and CH2O has been made by the GOME instrument on ERS-2. The prime advantage of satellites is their capability of providing a full global mapping of the atmospheric composition. After cloud filtering, GOME provides global coverage tropospheric NO2 and CH2O maps roughly every week. SCIAMACHY provides less coverage, but detects more detailed information due to its better spatial resolution than GOME. SCIAMACHY observations of tropospheric pollution are envisaged to contribute to model predictions of the chemical state of the atmosphere (chemical weather forecasting).

Column amounts of NO2 can be derived from the detailed spectral information provided by GOME and SCIAMACHY in the wavelength range 420-450 nm. Good signal-to-noise ratios (of about 20) are obtained for GOME NO2 with the Differential Optical Absorption Spectroscopy (DOAS) retrieval technique. This is related to the absence of strong other absorbers (e.g. ozone) in this spectral interval. GOME has also, demonstrated the ability to observe boundary layer NO2 [i.e. *Leue et al.*, 2001]: on top of a stratospheric background enhanced column NO2 amounts are observed that correlate well with known industrialised areas. GOME has also detected NO2 plumes originating from biomass burning events and enhanced CH2O concentrations over forests [*Palmer et al.*, 2001]. Furthermore, there are signatures of lightning-produced NO2 in the GOME data set [*Beirle et al.*, 2004].

2. FORWARD MODEL AND INVERSION PROCEDURE

There is a suit op papers describing retrieval techniques for total and tropospheric column NO2 [*Velders et al.*, 2001, *Martin et al.*, 2002, *Lauer et al.*, 2002 and *Richter and Burrows*, 2002] and CH2O [*Chance et al.*, 2000]. The method described here differs from most papers in the sense that a data-assimilation technique is used to estimate the stratospheric part of the NO2 column, which is an essential step in determining quantitatively accurate tropospheric and total NO2 columns. The reader is referred to *Eskes et al.* [2003] and *Boersma et al.* [2004] for more detailed information on this retrieval aspect. The technique used to determine CH2O will be quite similar as described in *Palmer et al.* [2001] and will not be discussed in more detail here. Below, an overview of the NO2 retrieval technique is given together with improvements over previous retrievals.

The first step in retrieving tropospheric NO2 is performed by BIRA-IASB and covers the spectral fitting of SCIAMACHY Lv1 data to generate so-called slant column densities (scd's) of NO2. These scd's will then be matched to KNMI FRESCO cloud parameters to obtain a pre-processed input dataset for the complete retrieval scheme.

2.1 Retrieval method slant columns

The technique used to retrieve total slant columns of atmospheric trace species from Satellite (GOME, SCIAMACHY) measurements is the Differential Optical Absorption Spectroscopy (DOAS). Differential Optical Absorption Spectroscopy is a widely used method to determine concentrations of atmospheric species [*Platt, 1994*]. The DOAS analyse of broadband spectra in the UV and visible region (200-800 nm) allows the determination of concentrations of atmospheric species, which leave their absorption fingerprints in the spectra.

The DOAS technique is based on a straightforward implementation of the Beer-Lambert's law, which describes the extinction of the solar radiation in an absorbing atmosphere:

$$I(\lambda) = I_0(\lambda).\exp(-\sum_i \sigma_i c_i) \qquad [4.1]$$

where : $I(\lambda)$ is the solar spectrum after absorption (earthshine radiance);

$I_0(\lambda)$ is the extraterrestrial solar spectrum (solar irradiance);

σ_i are the relevant cross sections of the absorbing species, with wavelength and temperature dependent structures;

c_i are the unknown species column densities.

The logarithm of the ratio of the irradiance spectrum $(I_0(\lambda))$ and the earthshine spectrum $(I(\lambda))$ is denoted optical density (or optical thickness):

$$\log(I_0(\lambda) - I(\lambda)) = \sum_i \sigma_i c_i \qquad [4.2]$$

The DOAS approach is a direct application of equation 4.2. High frequency spectral structures characteristics of the various absorbing species are used to resolve the corresponding contributions to the total optical density. This is obtained using a least-square procedure where the slant column densities (SCD) of the various species are the fitted parameters. Large band contributions to the atmospheric attenuation (Rayleigh and Mie scattering) are accounted for by a low order polynomial function. Simply stated, the DOAS technique is a linear problem. This linearity is however broken down by the need to account for additional effects, namely:

- small wavelength shifts between I and I_0 spectra must be corrected using appropriate shift and stretch parameters,
- possible instrumental and/or atmospheric straylight or residual dark current signal require the introduction of an offset parameter.

In addition to shift and offset, Ring and undersampling effects have to be treated. The so-called Ring effect arises in the atmosphere due to inelastic scattering processes (mainly Rotational Raman Scattering (RRS) by molecular O_2 and N_2). Roughly speaking, it manifests itself by a broadening of the solar and atmospheric spectral features present in the satellite earthshine backscattered spectra. This broadening typically reduces the depth of thin solar and atmospheric absorption features by several percents. Hence, it has a strong impact on spectroscopic measurements using the DOAS method and requires appropriate correction to be implemented in retrieval algorithms. In DOAS, the Ring effect is usually accounted for as an absorber. Ring cross sections can be obtained from different sources [*Vountas*, *1998*], [*Chance*, *1997*].
The undersampling problem arises from the poor sampling ratio of the instrument which results in a lost of spectral information when interpolating earthshine spectra during the DOAS fitting process. To some extent, the problem can be corrected by using an ad-hoc cross section obtained by simulating the effect based on a high-resolution solar reference.

Let us consider the modified equation:

$$\log(I(\lambda + \Delta\lambda) - \mathit{offset}(\lambda)) = \log(I_0(\lambda)) - \sum_i \sigma_i(\lambda) c_i - P - \sigma_{ring}(\lambda) c_{ring} - \sigma_u(\lambda) c_u \qquad [4.3]$$

P is the polynomial. Undersampling cross section and ring effect cross section are simply included as additional pseudo-absorbers.

The selection of the spectral analysis window determines which absorbers have to be included in the fitting procedure. Several cross sections of a same absorber can be fitted together (for example to account for a temperature dependency of the cross sections).

Residuals of equation 4.3 are minimised using a Marquardt-Levenberg non-linear least-squares (NLLS) algorithm. The method implements a gradient-expansion algorithm, which is based on the iterative combination of a steepest-descent method (suitable for approaching the minimum from far away) and a linearization of the fitting function. Linear parameters are determined by a Singular Value Decomposition (SVD) method embedded in the NLLS algorithm.

The DOAS Software

The DOAS of spectra is performed using **WinDOAS**, a multi-purpose DOAS analysis software developed over the nineties at BIRA-IASB. This software initially developed for ground-based applications has been thoroughly validated through participation at various intercomparison exercises [*Hofmann, 1995*], [*Roscoe, 1999*], [*Aliwell, 2002*]. For more information on the algorithm details, see the "*WinDOAS 2.1* Software User Manual" [*Fayt, Van Roozendael*] (http://uv-vis.aeronomie.be/software/WinDOAS/).

Overview SCIAMACHY NO_2 Slant Columns Retrieval

Software:	**WINDOAS** [*Fayt, Van Roozendael, 2001*]
Analysis Method:	Differential Optical Absorption Spectroscopy
Fitting interval:	426.3 - 451.3 nm (channel 3, cluster 15)
Molecular absorption cross-sections:	NO_2 at 243K [*Bogumil et al., 1999*] O_3 at 223K [*Bogumil et al., 1999*] O_4 [*Greenblatt et al., 1990*] H_2O [*Rothman, 1992*]
Additional terms/corrections:	Calculated ring spectrum [*Vountas, 1998*] Polynomial (order 2) Offset (constant + slope)

A radiance reference spectrum over Indian Ocean is used, where the tropospheric NO_2 is supposed to be almost zero. A stratospheric correction is applied afterwards, taking into account the SZA of the reference spectrum and the stratospheric NO_2 VCD in this region ($1.5\text{x}10^{15}$) [*Lambert, 2002*].

2.2 Conversion of slant columns to total columns

The slant column (N_s) calculated with the DOAS method can be converted to the vertical column (x) by applying the air mass factor (M):

$$x = \frac{N_s}{M(\mathbf{x_a}, \mathbf{b})} \qquad [4.4],$$

The air mass factor is calculated with the DAK radiative transfer model [*Stammes*, 2000] and depends on the *a priori* profile shape ($\mathbf{x_a}$) and the model parameters ($\mathbf{b}$). See the discussion on the tropospheric air mass factor in the next section for a detailed description.

2.3 Retrieval method tropospheric columns

The retrieval approach for tropospheric columnar NO2 in TEMIS is the DOAS method. This method consists of two steps:

(1) The retrieval of slant columns as described above in section 1.1.

(2) The application of an air mass factor to convert the slant column into a vertical column. For practical applications of DOAS it is important that the trace gas under investigation has a small absorption optical thickness in the predefined spectral window. For example, NO2 has a typical slant optical thickness of 0.005.

The method described above is principally used for total column retrievals. However, NO2 permanently resides in the stratosphere, and shows significant amounts in the troposphere near source areas. Our retrieval method first separates the stratospheric and tropospheric part of the column, and subsequently a tropospheric air mass factor is applied to the tropospheric slant column:

$$x_{tr} = \frac{N_s - N_{s,st}}{M_{tr}(\mathbf{x_a}, \mathbf{b})} \qquad [4.5],$$

where N_s denotes the slant column density as obtained from step 1 as described above, $N_{s,st}$ is the stratospheric component of the slant column, and M_{tr} represents the tropospheric air mass factor. The tropospheric air mass factor depends on the a priori profile shape $\mathbf{x_a}$ and the set of model parameters $\mathbf{b}$.

One of the innovations of the retrieval method applied in the TEMIS project is that the stratospheric part of the slant column is determined by data assimilation of observed slant columns in a chemistry-transport model proposed and described in *Eskes et al.*, [2003]. Shortly summarized, SCIAMACHY slant column observations are assimilated in TM4 as follows:

- A priori NO2 profiles are convolved with the averaging kernel (obtained with the DAK radiative transfer model [*Stammes*, 2000]) to give the model predicted slant column densities ($N_{s,m} = \mathbf{A} \cdot \mathbf{x_a} / M$, with $N_{s,m}$ the model predicted slant column, and $\mathbf{A}$ the averaging kernel).
- The differences between the observed and modelled columns are used to force the modelled columns to generate an analysed state based on the model forecast and GOME observations. This forcing depends on weights (from observation representativeness and model errors) attributed to both modelled and observed columns. Observed columns are attributed a low weight if the model predicts large tropospheric columns. This reflects the uncertainty in the averaging kernel, and minimises the influence of slant columns contaminated by tropospheric signals. The forcing equation is solved with the statistical interpolation method, involving a covariance matrix operator that incorporates the assumed 3-D correlation of NO2 differences. The most important characteristics of this forecast covariance matrix are; (1) the conservation of model profile shapes, i.e. differences between modelled and observed quantities are not vertically redistributed but rather scaled in the forcing equation, and (2) the horizontal correlation model function is assumed to follow a Gaussian shape with a 1/e correlation length of 600 km.
- The forecast field is subsequently replaced by the analysis. This cycle is repeated for all available orbits.

The advantage of the approach is that slant column variations due to stratospheric dynamics are now accounted for. The aim is to decrease the accuracy threshold of tropospheric columns that can be retrieved. An additional advantage is that the assimilation scheme provides a statistical estimate of the uncertainty in the stratospheric slant column.

The tropospheric air mass factor M_{tr} is obtained by multiplying the elements of the troposphere-only a priori NO2 profile $\mathbf{x}_\mathbf{a}$ derived from chemistry-transport model TM4 with the elements of the altitude dependent air mass factor m_l as follows:

$$M_{tr} = \frac{\sum_l m_l(\mathbf{b}) \cdot x_{a,l}}{\sum_l x_{a,l}} \qquad [4.6],$$

and where the elements of the altitude dependent air mass factor depend on the set of model parameters **b** including cloud fraction, cloud height and surface albedo.

The air mass factor can be written as [*Boersma et al.*, 2004]:

$$M_{tr} = M(\mathbf{x}_\mathbf{a}, \mathbf{b}) = M(\mathbf{x}_\mathbf{a}, f_{cl}, z_{cl}, a_{sf}, \boldsymbol{\tau}_\mathbf{aer}) \qquad [4.7],$$

where f_{cl} is the cloud fraction, z_{cl} is the cloud (top) height, a_{sf} is the surface albedo, and $\boldsymbol{\tau}_\mathbf{aer}$ is the aerosol optical thickness profile. The air mass factor depends on the solar zenith, viewing zenith and relative azimuth angle as well, but the measurement geometry is known with high accuracy and therefore does not contribute significantly to the error in the air mass factor. Each of the contributions of f_{cl} , z_{cl} , a_{sf} and $\boldsymbol{\tau}_\mathbf{aer}$ to the error in the air mass factor is extensively discussed by *Boersma et al.* [2004].

For the fit of slant column a fixed temperature of 243K has been used for the cross-section. However, the cross-sections are temperature dependent. To correct for this, an empirical correction factor has been used in the air mass factor calculation.

3. AUXILIARY DATA

For the tropospheric NO_2 algorithm the following auxiliary data is needed: ECMWF meteorological fields, surface albedo climatology (Combined TOMS-GOME albedo climatology), topology database (GTOPO30), and emission databases (EDGAR etc). The data is specified below.

3.1 Specification of the ECMWF operational analyses

Originating System:	ECMWF
Data Class	Model
Name of Data Source	OD (Operational ECMWF-IFS analyses)
Sensor Type/Name:	N/A
Sensor key technical parameters	
Spatial resolution / coverage: TL511 Vertical resolution / coverage: 60 layer Temporal resolution / coverage: 3h/6h	
System operations availability	
Start date: January 2000 End date: present	
Probability of availability	
100 %	
Product name and reference to product technical specification document:	
ECMWF-OD. Documentation at http://www.ecmwf.int	
Data availability and coverage:	
Time-scale: 6 hours after acquisition Geographic: Global	
Quality and reliability:	
Quality: High **Reliability:** 100 %	
Further parameters and remarks:	
Wind, temperature, pressure.	
References:	
• Different aspects of the ECMWF IFS are discussed in technical memos and reports available from the ECMWF web site, http://www.ecmwf.int/.	

3.2 Specification of the GTOPO30 climatology

Originating System:	U.S. Geological Survey's EROS Data Center
Data Class	Climatology
Name of Data Source	GTOPO30
Sensor Type/Name:	N/A
Sensor key technical parameters	
Spatial resolution / coverage: 30-arc seconds Vertical resolution / coverage: N/A Temporal resolution / coverage: N/A	
System operations availability	
Start date: N/A End date: N/A	
Probability of availability	
100 %	
Product name and reference to product technical specification document:	
GTOPO30. Documentation at http://edcdaac.usgs.gov/gtopo30/README.asp	
Data availability and coverage:	
Time-scale: N/A Geographic: Global	
Further parameters and remarks:	
-	
References: http://edcdaac.usgs.gov/gtopo30/gtopo30.asp	

3.3 Specification of combined GOME/TOMS albedo climatology

Originating System:	TOMS and GOME data
Data Class	climatology
Name of Data Source	Albedo climatology from TOMS and GOME observations
Sensor Type/Name:	TOMS and GOME

Sensor key technical parameters
Spatial resolution / coverage: 1 x 1 degree / Global Vertical resolution / coverage: N/A Temporal resolution / coverage: N/A
System operations availability
Start date: N/A End date: N/A
Probability of availability
100 %
Product name and reference to product technical specification document:
TOMS albedo data set : see GSE-PRO-IN-EO-5 and *Herman, J. R. and E. A. Celarier, Earth surface reflectivity climatology at 340-380 nm from TOMS data, J. Geophys. Res., 102, 28,003-28,011, 1997.* GOME albedo data set : *Koelemeijer, R. B. A., P. Stammes, J. W. Hovenier, and J. F. de Haan, Global distributions of effective cloud fraction and cloud top pressure derived from oxygen A band spectra measured by the Global Ozone Monitoring Experiment: comparison to ISCCP data, J. Geophys. Res., 107(D12), 4151, doi: 10.1029/2001JD000840, 2002.*
Data availability and coverage:
Time-scale: N/A Geographic: Global
Further parameters and remarks:
-
References:

3.4 Specification of emission databases EDGAR/GEIA

Other Data Sources	
Originating System:	EDGAR, GEIA
Data Class	Emission climatology
Name of Data Source	EDGAR and GEIA emission inventories
Sensor Type/Name:	-
Sensor key technical parameters	
Spatial resolution / coverage: 1 x 1 degree / Global Vertical resolution / coverage: N/A Temporal resolution / coverage: Annual totals	
System operations availability	
Start date: N/A End date: N/A	
Probability of availability	
100 %	
Product name and reference to product technical specification document:	
EDGAR v2 : see *Olivier et al, RIVM report 771060, Natl. Inst. Of Public Health and Environ., Bilthoven, Netherlands, 1996.* *Benkovitz et al, JGR 101, 29239, 1996.* *Guenther et al, JGR 100, 8873, 1995* *Yienger and Levy, JGR 100, 11447, 1995.*	
Data availability and coverage:	
Time-scale: N/A Geographic: Global	

4. SENSITIVITY AND ERROR ANALYSIS

The previous section illustrated the most important dependencies of NO_2 retrieval. Accurate quantitative estimates are needed for instance for quantitative regional air pollution monitoring, pollution trend studies and budget calculations, and realistic quantitative estimates of the columns and their errors are essential and should be given for every individual retrieval. Furthermore, this type of retrieval method is relatively young, and usually not validated. One step in convincing users that tropospheric columns are quantitative and accurate, is to provide realistic uncertainty estimates along with the columns.

For a detailed discussion on the error analysis approach taken in the TEMIS project, the reader is referred to *Boersma et al.* [2004]. Below a short summary is given of the current knowledge of the most important error sources in the retrieval of tropospheric NO2 columns:

- Errors in the slant column density (step 1). These are estimated from the uncertainty on the fit parameter for NO2 in the SCIAMACHY DOAS retrieval. A systematic error in N_s is expected as a consequence of the use of an Earthshine spectrum instead of a Solar irradiance spectrum but in first order, this is corrected for.
- Errors in the stratospheric slant column density. These errors are estimated from the standard deviation of the differences between model forecast and observed stratospheric NO2. Note that if a systematic error is present in N_s, that this will also be present in $N_{s,st}$, and thus cancels in the determination of the tropospheric part of the slant column (N_s -$N_{s,st}$).
- Errors in the tropospheric air-mass factor. In our method, there are four contributions to the overall uncertainty in the tropospheric air mass factor; cloud fraction, cloud height, surface albedo, and a priori profile shape. Cloud errors are very important since clouds shield near-surface NO2 from the satellite's view. The tropospheric air mass factor is very sensitive to clouds and even small cloud fractions (up to 20%) have a major impact. The tropospheric air mass factor is also very sensitive to the surface albedo especially when little clouds are present. The last and least understood error source is the a priori profile shape (and representativeness errors). Given the lack of measured tropospheric NO2 profile shapes, predictions by a CTM are currently the best option. CTM TM4 contains arguably realistic emission estimates as well as chemistry, and is equipped with vertical and horizontal transport derived from ECMWF meteorology. Nevertheless, there are some important uncertainties related to the predicted profile shapes, such as the undersampling of the model (2.5º x 2.5º, i.e. 250 x 200 km^2 at mid-latitudes) relative to the SCIAMACHY pixel size of (30 x 60 km^2), leading to representativeness errors.

In summary, the TEMIS total and tropospheric NO_2 products will be provided with error estimates based on the error sources discussed above. Error estimates will be given on a quantitative and pixel-to-pixel basis. However, in order to fully understand the retrieved quantitative columns, we note here that a thorough validation effort is required. Repeatedly measured NO_2 profile shapes will be of great use in determining the impact of the a priori profile shape in the retrieval approach.

4.1 Averaging kernels

In *Boersma et al.* [2004], the importance of the a priori profile shape was extensively discussed. It was shown that the tropospheric air mass factor critically depended on the a priori profile shape and that the choice for a particular profile is an important source of error. Within the TEMIS project, averaging kernels are provided. Kernels describe how the retrieved vertical column is related to the a priori profile $\mathbf{x_a}$, i.e.

$$N_v = \mathbf{A} \cdot \mathbf{x}_a \qquad [4.6],$$

or, written differently, how the measured slant column is related to the true profile $\mathbf{x_t}$:

$$N_s = m_l(\mathbf{b}) \cdot \mathbf{x_t} \qquad [4.7].$$

Furthermore, the kernels are crucial for a detailed understanding of individual observations. The elements of the averaging kernel itself are written out as follows:

$$A_l = \frac{m_l(\mathbf{b})}{M(\mathbf{x_a})} \qquad [4.8],$$

or, in words, the elements of the averaging kernel vector are equal to the elements of the altitude dependent air mass factor divided by the total air mass factor. These averaging kernel elements are given in the TEMIS data product.

Applications of the averaging kernel include

- Validation: equation 4.7 allows a direct comparison of measured NO2 profiles $\mathbf{x}$ to satellite measured slant columns N_s.
- Data-assimilation: here too the averaging kernel has the function of observation operator to translate a model predicted NO2 profile $\mathbf{x}$ to an apparent ‘modelled’ observation N_s.

5. ALGORITHM VALIDATION

5.1 The DOAS Software

The software used for the DOAS of spectra (WinDOAS) was initially developed for ground-based applications has been thoroughly validated through participation at various intercomparison exercises [*Hofmann, 1995*], [*Roscoe, 1999*], [*Aliwell, 2002*]. For more information on the algorithm details, see the "*WinDOAS 2.1* Software User Manual" [*Fayt, Van Roozendael*] (http://uv-vis.aeronomie.be/software/WinDOAS/).

5.2 Preliminary results of geophysical validation

A few SCIAMACHY NO_2 products, where among the TEMIS NO_2 product, have been validated by *Lambert et al* [2004]. The preliminary results of this validation have been presented at the ACVE-2 meeting in 2004. A citation of Lambert's results regarding the TEMIS NO_2 product follows.

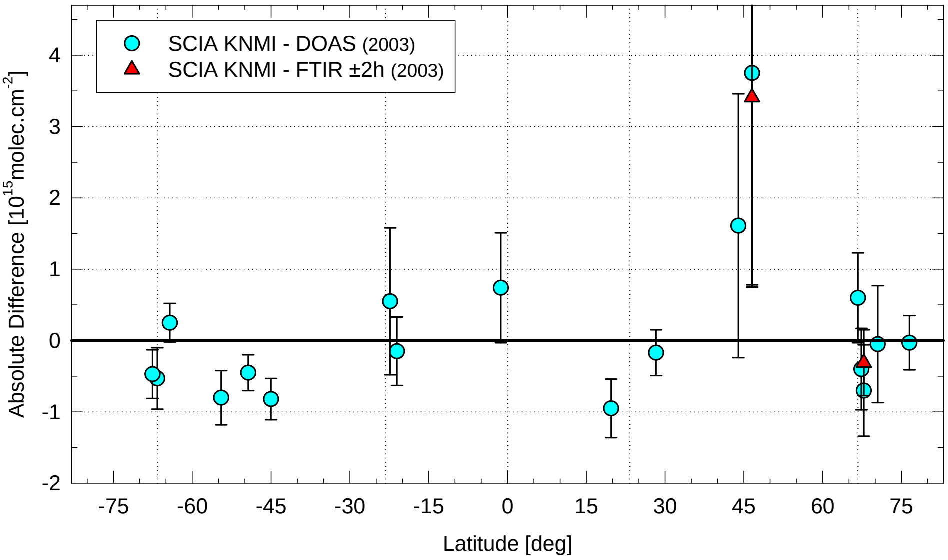

Figure 3.1 *– Meridian variation of the mean absolute difference between near real time total nitrogen dioxide in July/November 2002 as reported by NDSC ground-based spectrometers and by the SCIAMACHY NO_2 slant columns retrieved from raw level-1 data by the research processor developed at BIRA-IASB, converted into vertical columns by KNMI. (source: Lambert et al.)*

"The pole-to-pole comparison between NDSC NO_2 data and the SCIAMACHY data set generated at KNMI/BIRA is depicted in Figure 3.1. The main difference is observed at polluted sites of the Northern middle latitudes where the discrepancy between SCIAMACHY and NDSC data reaches values as high as $3.5\ 10^{15}$ molec.cm^{-2}. According to modelling results and (unfortunately non correlated) airborne measurements, such high values would be better estimates of the tropospheric NO_2 column. Such a difference between KNMI/BIRA retrievals and retrievals of other institutes is supposed to come mostly from the use of tropospheric AMF. GOME and SCIAMACHY total NO_2 retrievals using a pure stratospheric AMF are known to underestimate the vertical column in the presence of tropospheric NO_2. Usually limited to 10% to 30%, this underestimation can reach a factor of two under extreme conditions. Another likely source of discrepancy, explaining the difference in behaviour at the stratospheric reference stations of the southern middle latitudes, comes from the use of a correction factor to account for the temperature dependence of the NO_2 absorption cross-sections. DAK RTM-computed AMFs approach geometrical AMF values in the clean Southern mid-latitude case. However, the total AMF used in the retrieval is the product of this quasi-geometrical AMF by the temperature correction based on ECMWF analyses. Studies indicate that stratospheric temperatures are typically about 15K lower than the temperature of the cross section used in the DOAS fit (243K, SCIA PFM). The typical NO_2 correction applied for such a temperature difference is about -5%, which corresponds to an increase in the reported AMF of 5%. Further quantitative interpretation of the results depicted in Figure 3.1 should take into account also how the temperature effect is taken into account in the retrieval of ground-based NDSC data.”

5.3 Model comparison

In this section, the comparison between SCIAMACHY NO_2 tropospheric columns and corresponding outputs of the regional chemical-transport model CHIMERE will be shown.

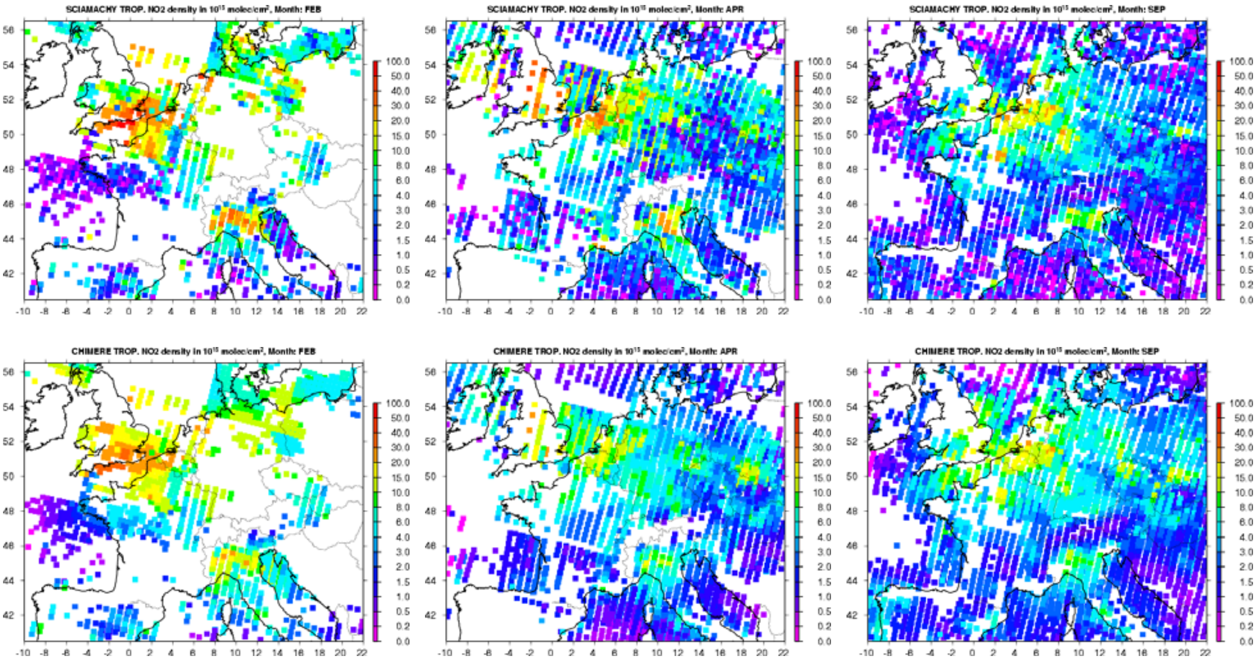

Figure 3.2 *Comparisons between daily NO_2 tropospheric columns retrieved from SCIAMACHY and that of issued from CHIMERE continental simulations. a)b)c) mean SCIAMACHY NO_2 tropospheric columns respectively for 24/01/2003, 14/02/2003, 25/09/2003. d)e)f) corresponding maps issued from CHIMERE. Unity in 10^{15}molecules/cm^3.*

Figure 3.2 shows that CHIMERE outputs and SCIAMACHY measurements are consistent in monthly averages. Only cloud free pixels are presented. The model is able to simulate the observed NO_2 patterns on the continent but also over the sea (Figures 3.2a and 3.2d). Observations over sea contain new information. In Figures 3.2a and Figure3.2d, two NO_2 plumes are visible: one between France and England that is mostly due to the pollution in the south-east of England and that of Benelux (this situation happens on 14/02/2003, Figures 3.3b and 3.3e.), the other one is located in the north-east of England, coming from The Netherlands.

Statistic values are calculated for a comparison between NO_2 tropospheric columns retrieved from SCIAMACHY and that from CHIMERE continental simulations. The table below details the statistic values of the comparison of daily averages for each month in 2003. The correlation coefficient shows the spatial consistency in the data. N(obs) corrresponds to the number of observation data. There was no data in November. The unity is 10^{15}molec./cm^3

Date	Bias	RMS	Correlation	Mean_obs	Mean_model	N(obs)
January	2.4	4.0	0.75	5.4	7.8	709
Febuary	0.5	5.1	0.80	8.1	8.6	1311
March	1.1	3.2	0.70	3.4	4.5	2347
April	-1.4	4.0	0.72	5.5	4.2	2635
May	-0.7	2.6	0.71	3.5	2.7	2797
June	-0.6	2.2	0.69	3.0	2.4	4519
July	0.1	2.1	0.71	2.8	2.8	3334
August	-0.2	1.7	0.72	2.8	2.6	2492
September	0.7	2.0	0.80	2.9	3.6	3513
October	1.8	3.0	0.74	3.0	4.9	2651
December	2.6	4.9	0.65	4.7	7.3	492
All data	0.2	2.9	0.73	3.6	3.8	26800

Figure 3.3 illustrates a comparison on daily basis, showing a very good agreement of the data. This last comparison demonstrates the ability of SCIAMACHY data to follow air pollution events and to point out problems in emission inventories. In this case, we didn't use a cloud mask (i.e. all of the pixels are presented). In this way, also plumes above the clouds can be seen, which is the case on 14 Febuary 2003 over the Atlantic ocean (Figure 3.3b). This shows that by using a cloud mask, essential information may be lost.

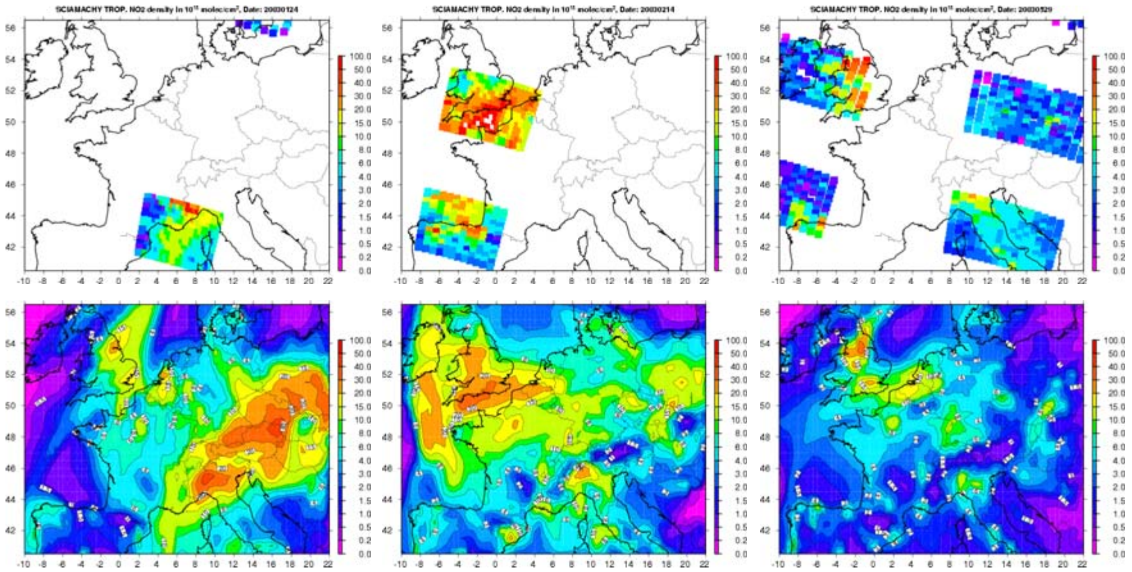

Figure 3.3 *Comparisons between daily NO_2 tropospheric columns retrieved from SCIAMACHY and that of issued from CHIMERE continental simulations. a)b)c) mean SCIAMACHY NO_2 tropospheric columns respectively for 24/01/2003, 14/02/2003, 25/09/2003. d)e)f) corresponding maps issued from CHIMERE. Unity in 10^{15}molecules/cm^3.*

5.4 Intercomparison with ground-based DOAS

Here we considered measurements performed from March to September 2003. The covered period involves large natural and human induced variation in tropospheric NO2 and represents thus a good test for the intercomparison. In figure 4.1.2.2 a scattered plot of the selected simultaneous measurements between SCIAMACHY and GACOD spectrometers is shown on the left part.

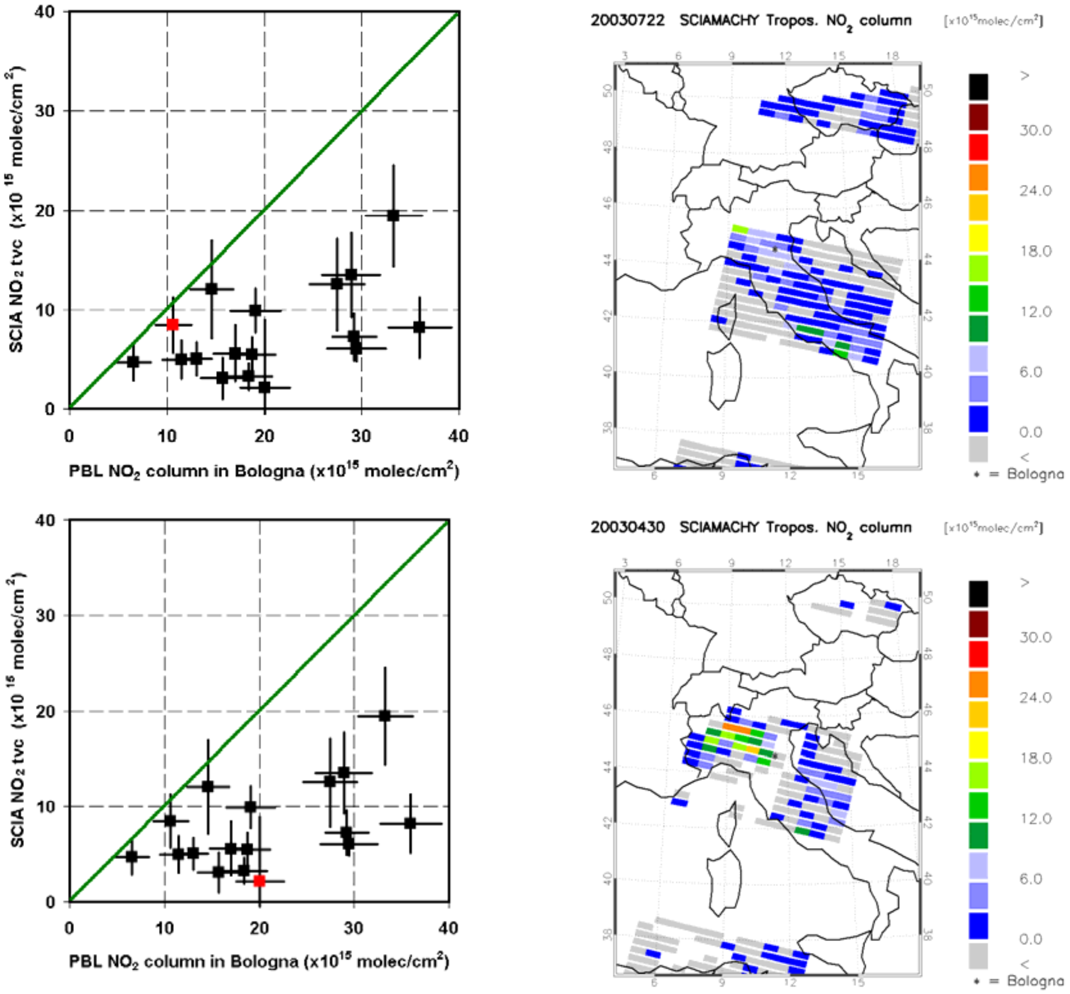

***Figure 4.2.1**: Scatter plot of SCIAMACHY NO2 tropospheric column versus the NO2 PBL column retrieved in the Bologna area from March to September 2003 (left part). Red squares refer to the values observed on the July 22nd (upper plot) and April 30th for which the respective SCIAMACHY observations in the all Po valley area is reported on the right part of the plot.*

All the data points lay in the part of NO_2_PBL > SCIA_NO_2 except three days for which the NO2 tropospheric column measurements are in agreements within the error bars. The main reason for this behaviour has been explained in Petritoli et al. [2004] that is the NO2_PBL column is observed near the pollution sources and thus should represent a sort of the maximum concentration that can be present within the SCIAMACHY pixel at the overpass. When tropospheric NO2 is well mixed in the area of the SCIAMACHY pixel (the case July 22nd for example in the upper part of figure 4.1.2.2) the agreement between the observations from the two instruments is good but if this is not the case (April 30th for example, in the lower part of figure 4.1.2.2) SCIAMACHY measures a sort of average of the NO2 column distribution within its field of view. This causes the difference between the two observations.

5.5 Recommendations for product validation

In order to make a proper comparison between ground-based measurements and satellite retrievals, knowledge on the actual tropospheric NO_2 profile and the horizontal distribution on ground pixel scale is needed. In addition, the assumptions used in the retrieval should be verified, with respect to clouds, aerosol, stratospheric NO_2 and albedo. Validation measurements therefore ideally should be done with several independent NO_2 measuring devices (in-situ vs remote, column vs profile) and with additional instrumentation to measure relevant atmospheric conditions. The use of high resolution models should complete our knowledge on stratospheric and tropospheric profiles, temporal variations due to transport and (photo-)chemistry, and should aid with the conversion from point to pixel measurement.

6. REFERENCES

Aliwell, S.R., M. Van Roozendael, P. V. Johnston, A. Richter, T. Wagner, et al., "Analysis for BrO in zenith-sky spectra - An intercomparison exercise for analysis improvement," J. Geophys. Res., 2002, doi:10.1029/2001JD000329.

S. Beirle, U. Platt, M. Wenig, T. Wagner, NOx production by lightning estimated with GOME, Advances in Space Research, Volume 34, Issue 4, Trace Constituents in the Troposphere and Lower Stratosphere, 2004, Pages 793-797, ISSN 0273-1177, DOI: 10.1016/j.asr.2003.07.069.

Blond, N., K.F. Boersma, H.J. Eskes, R.J. van der A, M. Van Roozendael, I. De Smedt, G. Bergametti and R. Vautard, Intercomparison of SCIAMACHY nitrogen dioxide observations, in situ measurements and air quality modeling results over Western Europe, J. Geophys. Res., 2007, 112, doi:10.1029/2006JD007277.

Boersma, K. F., H. J. Eskes, and E. J. Brinksma, Error Analysis for Tropospheric NO2 Retrieval from Space, *J. Geophys. Res.*, 2004.

Bogumil, K., J. Orphal and J. P. Burrows: Reference Spectra Of Atmospheric Relevant Trace Gases Measured With The Sciamachy Pfm Satellite Spectrometer; Proc. 5th Colloquium "Atmospheric Spectroscopy Applications (Asa), Reims, France, 1999.

Chance, K. V., P. I. Palmer, R. J. D. Spurr, R. V. Martin, T. P. Kurosu, and D. J. Jacob, Satellite observations of formaldehyde over North America from GOME, *Geophys. Res. Lett.*, 27, 3461-3464, 2000.

Chance, K. and R.J.D. Spurr, Ring effect studies : Rayleigh Scattering, including molecular parameters for Rotational Raman Scattering, and the Fraunhofer Spectrum, Appl. Opt., 36, 5224-5230, 1997.

Eskes, H. J. et al., GOME assimilated and validated Ozone and NO2 fields for Scientific Users and Model Validation, Final Report (http://www.knmi.nl/goa), European Commission, Fifth Framework Programme, Environment and Sustainable Development, 1998-2002, April 2003.

Eskes, H. J., and K.F. Boersma, Averaging kernels for DOAS total-column satellite retrievals, *Atmos. Chem. Phys.*, 3, 1285-1291, 2003.

Fayt, C., Van Roozendael, M.:*WinDOAS 2.1* Software User Manual, 2001, http://uv-vis.aeronomie.be/software/WinDOAS/

Greenblatt G. D., J.J. Orlando, J.B. Burkholder, and A.R. Ravishankara: Absorption measurements of oxygen between 330 and 1140 nm, J. Geophys. Res., 95, 18577-18582, 1990.

Hofmann, D., et al.:Intercomparison of UV/Visible Spectrometers for Measurements of Stratospheric NO2 for the Network for the Detection of Stratospheric Change, J. Geophys. Res., Vol. 16, pp. 16,765-16,791, 1995.

Lambert,J.C.: Ground-based comparisons of SCIAMACHY NRT O3 and NO2 Columns, Envisat Validation Workshop, ACVT, GBMCD, 2002.

Lambert, J-C., J. Granville, T. Blumenstock, F. Boersma, A. Bracher, M. De Mazière, P. Demoulin, I. De Smedt, H. Eskes, M. Gil, F. Goutail, F. Hendrick, D. V. Ionov, P. V. Johnston, I. Kostadinov, K. Kreher, E. Kyrö, R. Martin, A. Meier, M. Navarro Comas, A. Petritoli, J-P. Pommereau, A. Richter, H. K. Roscoe, C. Sioris, R. Sussmann, M. Van Roozendael, T. Wagner, and T. Wood, Geophysical Validation of SCIAMACHY NO_2 Vertical columns: Overview of Early 2004 Results, proceedings ACVE-2 meeting, 2004

Lauer, A., M. Dameris, A. Richter, and J.P. Burrows, Tropospheric NO2 columns: a comparison between model and retrieved data from GOME measurements, *Atmos. Chem. Phys.*, 2, 67-78, 2002.

Leue, C., M. Wenig, T. Wagner, O. Klimm, U. Platt and B. Jaehne, Quantitative analysis of NOx emissions from GOME satellite image sequences, *J. Geophys. Res.*, 106, 5493-5505, 2001.

Martin, R.V., K.Chance, D. J. Jacob, T. P. Kurosu, R. J. D. Spurr, E. Bucsela, J. F. Gleason, P. I. Palmer, I. Bey, A. M. Fiore, Q. Li, R. M. Yantosca, and R. B. A. Koelemeijer, An improved Retrieval of Tropospheric Nitrogen Dioxide from GOME, , *J. Geophys. Res.*, 107, D20, 4437, 10.1029/2001JD001027, 2002.

Palmer, P. I., D. J. Jacob, K. Chance, R. V. Martin, R. J. D. Spurr, T. P. Kurosu, I. Bey, R. Yantosca, A. Fiore, and Q. Li, Air-mass factor formulation for spectroscopic measurements from satellites: application to formaldehyde retrievals from GOME, *J. Geophys. Res.*, 106, 14,539-14,550, 2001.

Petritoli A., Bonasoni P., Giovanelli G., Ravegnani F., Kostadinov I., Bortoli D., Weiss A., Schaub D., Richter A. and F. Fortezza (2004), First comparison between ground-based and satellite-borne measurements of tropospheric nitrogen dioxide in the Po basin, J. Geophys. Res., Vol. 109, No. D15, D15307 10.1029/2004JD004547.

Platt, U., “Differential optical absorption spectroscopy (DOAS), Air monitoring by Spectroscopic Techniques (M. Sigrist, ed.)”, John Wiley & Sons, Inc., 1994, pp. 27–84.

Richter, A., and J. P. Burrows, Tropospheric NO2 from GOME measurements, *Adv. Space Res.*, 29, 1673-1683, 2002.

Roscoe, H.K., P.V. Johnston, M. Van Roozendael, A. Richter, J. Roscoe, et al., "Slant column measurements of O3 and NO2 during the NDSC intercomparison of zenith-sky UV-visible spectrometers in June 1996," J. Atmos. Chem., Vol. 32, 281-314, 1999.

Rothman, L.S.: The HITRAN data base, J. Quant. Spectrosc. Radiat. Transfer, 48, 5, 6, 1992.

Schaub, D., Weiss, A. K., Kaiser, J. W., Petritoli, A., Richter, A., Buchmann, B., and Burrows, J. P., A transboundary transport episode of nitrogen dioxide as observed from GOME and its impact in the Alpine region, *Atmos. Chem. Phys.*, 5, 23-37, 2005.

Stammes, P., Spectral radiance modelling in the UV-Visible range, in "IRS2000: Current Problems in Atmospheric Radiation", Eds. W.L. Smith and Y.M. Timofeyev, A. Deepak Publishing, Hampton (VA), 2000.

Velders, G. J. M., C. Granier, R. W. Portmann, K. Pfeilsticker, M. Wenig, T. Wagner, U. Platt, A. Richter, and J. P. Burrows, Global tropospheric NO2 column distributions: Comparing three-dimensional model calculations with GOME measurements, *J. Geophys. Res.*, 106, 12,643-12,660, 2001.

Vountas, M., V.V. Rozanov and J.P. Burrows, Ring effect: Impact of Rotational Raman Scattering on Radiative Transfer in Earth's Atmosphere, JQSRT, 60, 943, 1998.